World Academy of Science, Engineering and Technology
International Journal of Mechanical and Mechatronics Engineering
Vol:6, No:1, 2012

Elastic-Plastic Contact Analysis of Single Layer Solid Rough Surface Model using FEM

A. Megalingam and M.M.Mayuram

***Abstract*—**Evaluation of contact pressure, surface and subsurface contact stresses are essential to know the functional response of surface coatings and the contact behavior mainly depends on surface roughness, material property, thickness of layer and the manner of loading. Contact parameter evaluation of real rough surface contacts mostly relies on statistical single asperity contact approaches. In this work, a three dimensional layered solid rough surface in contact with a rigid flat is modeled and analyzed using finite element method. The rough surface of layered solid is generated by FFT approach. The generated rough surface is exported to a finite element method based ANSYS package through which the bottom up solid modeling is employed to create a deformable solid model with a layered solid rough surface on top. The discretization and contact analysis are carried by using the same ANSYS package. The elastic, elastoplastic and plastic deformations are continuous in the present finite element method unlike many other contact models. The Young's modulus to yield strength ratio of layer is varied in the present work to observe the contact parameters effect while keeping the surface roughness and substrate material properties as constant. The contacting asperities attain elastic, elastoplastic and plastic states with their continuity and asperity interaction phenomena is inherently included. The resultant contact parameters show that neighboring asperity interaction and the Young's modulus to yield strength ratio of layer influence the bulk deformation consequently affect the interface strength.

***Keywords*—**Asperity interaction, finite element method, rough surface contact, single layered solid

I. Introduction

CONTACT between rough surfaces affects the tribological properties like friction, wear and lubrication. The maximum contact pressure, real area of contact and surface and sub surface stresses influence the friction and wear of contacting rough surfaces, which are functions of surface roughness, surface stiffness and interfacial loading conditions. The multiple loading of mechanical components cause frequent surface contact interactions, which leads to the adhesive failure and subsurface failure in the contacting surfaces. So low contact pressure, small real area of contact and low surface and subsurface stresses are required to reduce friction, wear and failures. The deposition of thin layer in an effective manner can reduce the friction and wear rate without changing the base material property.

Several numerical models have been developed to analyze layered solid subjected to prescribed loading and boundary conditions. [1] presented a two dimensional theory for contact stresses between smooth and rough elastic cylinder. They considered three basic types of surface textures and also analyzed the effect of surface roughness on contact stresses for the case of soft layered, rough elastic cylinder in contact with a rough flat surface. In their analysis, the deflection was initially assumed then the contact pressure was calculated using Green function. [2] used Papkovinch-Neuber potentials to formulate a three dimensional problem for a rough surface in contact with a layered rough surface. A conventional matrix inversion technique was used to solve for the contact pressure and real contact area. First an initial contact area was determined from the geometrical interference, then an iterative process (calculate the contact pressure, modify the contact area by removing the areas with negative contact pressure) was repeated in a sequence until the results convergence. The conjugate gradient method [3,4] was employed to solve the system of linear equations which relate the contact pressure and displacements, for unknown contact pressures during the iterative process. These techniques can be used for rough surface contacts with a moderate number of contact points. [5] used variational principle for a homogeneous solid contact problem, to the frictionless contact analysis of a three dimensional rough surface against a nominally flat surface. According to a variational principle, the real area of contact and contact pressure distributions are those which minimize the total complementary potential energy. The Newton method was used to find the minimum total complementary potential energy. The variation principle approach was extended by [6] who used Papkovinch-Neuber potentials to derive the influence matrix of three dimensional single layered elastic/plastic rough surface contact model. The quasi-Newton method, a bounded constrained indefinite quadratic programming method was used to find the minimum total complementary potential energy. Finite element method based contact analysis of layered surface overcomes the difficulties of laborious numerical techniques and complex form of analytical formularizations. [7] provided a three dimensional finite element method based contact analysis of elastic-plastic layered media with fractal surface topography. They initially obtained a constitutive relation between mean contact pressure, real area of contact and corresponding representative strain for a finite element model of a rigid sphere in normal contact with a semi infinite elastic-plastic homogeneous medium. Then the constitute relation was modified for a layered medium to include the effects of mechanical properties of layers, substrate materials and the layer thickness. They used two variable Weierstrass-Mandelbrot function for three dimensional fractal surface generation. [8] presented a 2D plane strain finite element model for patterned elastic-plastic layered media to elucidate the effect of surface

Megalingam A is doctoral student at Department of Mechanical Engineering, Indian Institute of Technology Madras, Chennai - 600036 INDIA. (e-mail: mechmega@gmail.com).

Mayuram M M is Professor at Department of Mechanical Engineering, Indian Institute of Technology Madras, Chennai - 600036 INDIA (phone: +91-44-22574692, email: mayuram@iitm.ac.in).

geometry on the deformation and stress fields due to normal and sliding contact. Special contact elements were used to model the surface interaction between the layered media and a rigid asperity. Different meandered and sinusoidal surfaces were considered for layered media and resultant contact pressure distribution, surface tensile stress, and subsurface equivalent plastic strain were obtained. The significance of surface patterning on the deformation behavior was interpreted in terms of stress and strain results. Empirical relations for the contact pressure concentration factor and onset of yielding in the first hard layer were derived from finite element results for indented layered media with sinusoidal surface patterns.

Researchers have reported significant amount of work in the field of layered rough surface contacts. However, only a very few research works are available to explain the characteristics of layered solid rough surface contacts using finite element method. In this paper, a scale dependent three dimensional rough surface is generated using FFT technique then the generated rough surface data is transferred to a finite element method based ANSYS package. Using the same package, a single layer solid rough surface in contact with a rigid flat surface is developed. Contact analysis is carried out in the developed model with low and high stiffness layers. The resultant contact parameters and their causes are discussed in result and discussion section in detail.

II. Modeling Details

Generally, surfaces are defined using amplitude and spatial information. In order to simulate a real rough surface, surfaces having known autocorrelation function (ACF) and height distribution need to be generated. To accomplish this, two dimensional digital filter techniques are generally used [9]. The following steps are used to get a Gaussian rough surface [10]. An output sequence of *z(I, J)* for a known autocorrelation function by a two dimensional linear transformation system is defined as

$$z(I,J) = \sum_{k=0}^{n-1}\sum_{l=0}^{m-1} h(k,l)\eta(I-k, J-l) \quad (1)$$

Where, I =0, 1, 2… N-1, J=0, 1, 2… M-1,n =N/2,m =M/2
The Fourier transform of (1) is

$$Z(\omega_x,\omega_y) = H(\omega_x,\omega_y)A(\omega_x,\omega_y) \quad (2)$$

Where, A and Z are Fourier transformations of the input sequence η and output sequence Z respectively, and h is the transfer function of the system, defined by

$$H(\omega_x,\omega_y) = \sum_{k=0}^{n-1}\sum_{l=0}^{m-1} h(k,l)e^{-ikwx-ilwy} \quad (3)$$

The autocorrelation function of rough surfaces are generally taken as an exponential decay with coefficient set to give 10% at the specified correlation length, which can be expressed as

$$R_z(k,l) = s_q^{\,2}\exp\left\{-2.3\left[\left(\frac{k}{\beta_x}\right)^2+\left(\frac{l}{\beta_y}\right)^2\right]^{1/2}\right\} \quad (4)$$

Where, S_q is the standard deviation of the random surface heights, β_x and β_y are called the correlation lengths in x, y directions respectively. If $\beta_x=\beta_y=\beta$ then the surface is isotropic.

The power spectral density (PSD) function of the rough surface is obtained by the Fourier transform of R_z, is given by

$$S_z(\omega_x,\omega_y) = \frac{1}{nm}\sum_{k=-n/2+1}^{n/2-1}\sum_{l=-m/2+1}^{m/2-1} R_z(k,l)e^{-ik\omega_x}e^{-il\omega_y} \quad (5)$$

If $S_\eta(\omega_x\ \omega_y)$ is the PSD function of the input sequence, the relationship between S_η and S_z for a two dimensional linear system is

$$S_z(\omega_x,\omega_y) = \left|H(\omega_x,\omega_y)\right|^2 S_\eta(\omega_x,\omega_y) \quad (6)$$

Where, η is an input sequence composed of independent random numbers, so its PSD must be a constant. The inverse Fourier transform of $H(\omega_x, \omega_y)$ obtained from equation (6) gives the filter coefficients $h(k, l)$

$$h(k,l) = \frac{1}{nm}\sum_{\omega_x=-n/2+1}^{n/2-1}\sum_{\omega_y=-m/2+1}^{m/2+1} H(\omega_x,\omega_y)e^{-ik\omega_x}e^{-il\omega_y} \quad (7)$$

Now, $h(k, l)$ is obtained from (7) which can be used in (1) to get the output $z(I, J)$ with the specified ACF.

A matlab code is developed by using (1) to (7). Using the developed code, a 24μm×24μm Gaussian rough surface is created with an autocorrelation length of 0.5μm and a sampling interval of 1μm in x and y directions and a standard deviation of 0.01μm and the resultant rough surface is shown in Fig.1.

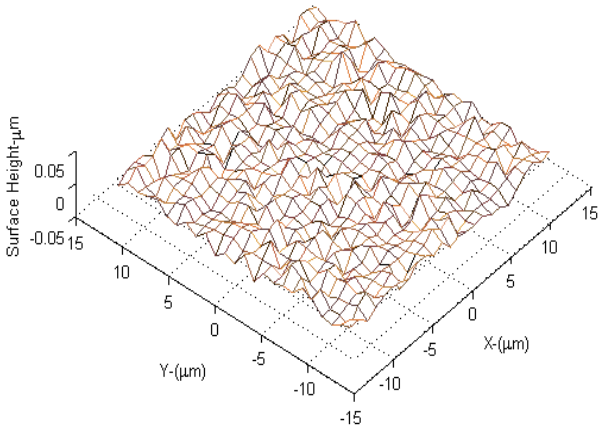

Fig. 1 Gaussian rough surface

III. Analysis Details

Surface altitudes z(x,y) of the generated Gaussian rough surface are imported as key points along with its x and y coordinate values in a finite element method package of ANSYS®. The imported key points are joined by splines, coons patch formulization is used to generate the rough surface. Bottom up solid modeling is used to create a deformable volume with the rough surface on top. Then the deformable volume is splitted into two halves by a splitting plane drawn at a distance, h/σ of 20.0 from the mean plane of surface and finally, the splitted volumes are glued in which the top deformable volume represents a coated layer as shown in Fig.2.The substrate volume has 8μm height which is enough to hold the bulk deformation. The deformable volumes are discretized with 10-node tetrahedral element (solid 92) with three degrees of freedom at each node. More than 70% of the elements are confined on the top portion of the single layer solid rough surface model as shown in Fig.3 to provide a converged result and to comfort the computational effort.

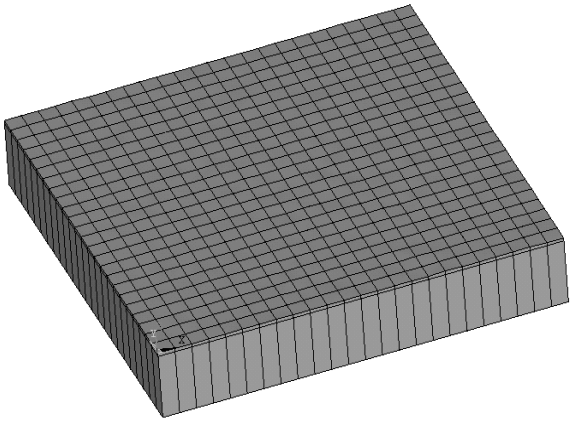

Fig. 2 Single layer solid rough surface model

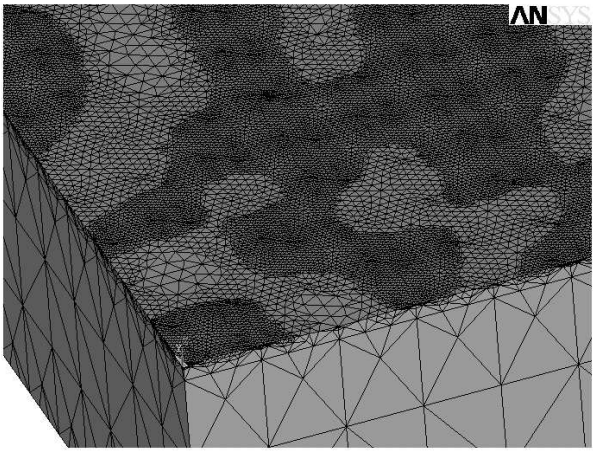

Fig. 3 Close view of discretized single layer rough surface model

A rigid flat surface is created over the discretized single layer rough surface model. Surface to surface contact pairs are developed between top rough surface and the rigid flat surface. CONTA 174 elements are made to lie over the deformable volume surface and TARGE 170 elements are used to discretize the rigid flat surface. Both CONTA 174 and TARGE 170 have 8 nodes each and are better suited for the contact of curved surfaces compared to other contact elements. To facilitate contact analysis of surface-to-surface contact elements, ANSYS provides either the augmented Lagrangian method or the penalty method. Here the augmented Lagrangian method is used which is an iterative series of penalty updates to find the exact Lagrangian multipliers and contact tractions. Compared to the penalty method, the augmented Lagrangian method usually leads to better conditioning of stiffness matrix and is less sensitive to the change in magnitude of the contact stiffness coefficient. The substrate material properties are E_2=100Gpa, γ_2=0.3 and H/E_2=0.05, selected from reference [11] and the material is assumed to behave in an elastic perfectly plastic manner. For the top layer, three relative material properties are used which E1/E2 of 2.0, 1.0 and 0.5 are keeping all other properties as substrate material properties. The nodes present at the bottom of the discretized model are constrained to move in all direction and the rigid flat surface is constrained to move in any direction except in vertical direction (along z direction).The displacements are applied on the rigid flat surface in an incremental manner to cover the entire asperity distribution in steps.

IV. Result And Discussion

The three cases of contact analyses are carried in small incremental step of interference. For all incremental steps of interference, total contact load is obtained by summing the nodal loads, total real area of contact is calculated by summing elemental areas which are in contact. The nodal pressure values are used to calculate maximum and mean contact pressures.Fig.4 shows the variation of dimensionless contact load with dimensionless interference. Till the dimensionless interference of 0.5, the deviation of dimensionless contact load is minimum due to few asperity contact which are all mostly in elastic state. As the interference increases, the asperities start to resist. In high stiff layer, the opposing load is high whereas in low stiffness layer this is low mainly due to the difference in the elastic property. In asperity level, the asperities of high stiffness layer have to withstand high load when compared to the low stiff layer for the same interference so the asperities of high stiffness layer enter into elastoplastic state in early compared to the asperities of low stiffness layer. This causes the high stiffness layer to bear high load bearing capacity. Fig.5 shows the variation of dimensionless real area of contact with dimensionless contact load. The high stiffness layer posses low bearing contact area in the whole deformation process compared to the low stiffness layer. During the initial interference, only few asperities are in contact which undergoes only elastic deformation and the contact load introduces a sharp raise in contact area mainly due to the elastically deforming asperities. Later, the increasing rate of contact area gets reduced because lot of asperities comes into contact and they start to interact among themselves.

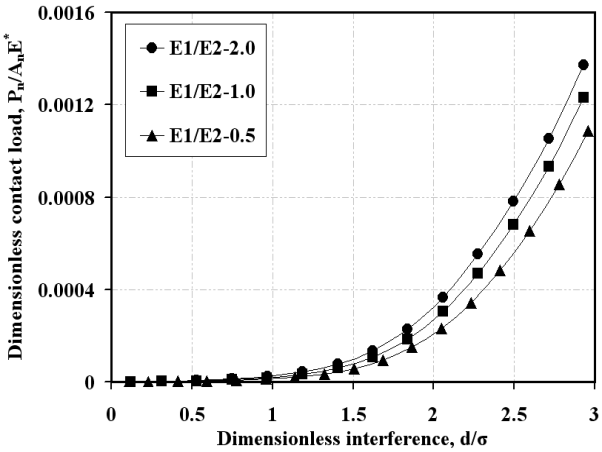

Fig. 4 Variation of dimensionless contact load with dimensionless interference

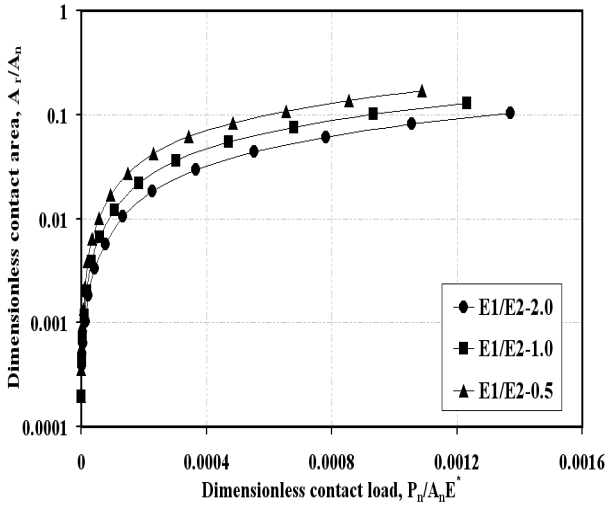

Fig. 5 Variation of dimensionless real area of contact with dimensionless contact load

Fig. 6 shows the variation of dimensionless mean contact pressure with dimensionless interference. During initial incremental interferences, few asperities come into contact and they deform elastically and show a linear variation in mean contact pressure ratio. Beyond the dimensionless interference of 0.6, the mean contact pressure ratio crosses the limit of 1.1Y denoted by Tabor [13] for the initial yielding so more number of asperities start to yield and the yielding occurs at the sub surface which affects the interface bonding strength of high stiffness layer. The effect of number of asperities under go elastoplastic and plastic deformation states can be seen in between the dimensionless interference of 0.6 to 2.0. Beyond the dimensionless interference of 2.0, almost all the asperities come into contact so the mean contact pressure ratio saturates at different level based on their layer stiffness.

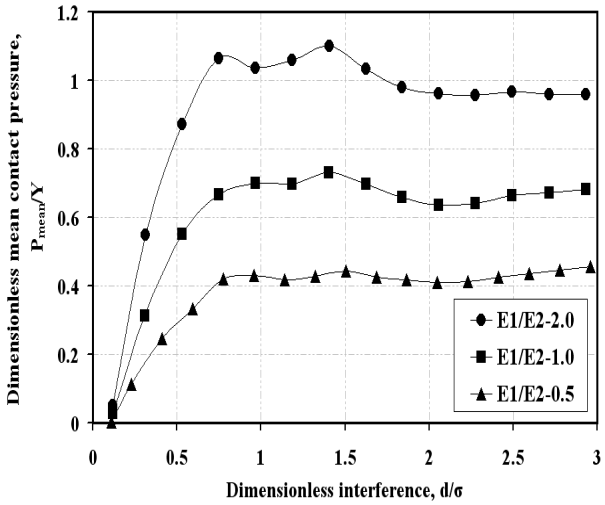

Fig. 6 Variation of dimensionless mean contact pressure with dimensionless interference

Fig. 7 shows the variation of dimensionless maximum contact pressure with dimensionless interference. The low stiffness layer case shows a clear gradually increasing trend as the dimensionless interference increases whereas the high stiffness layer case so some undulation in its trend mainly due to the influence of elastic, elastoplastic and plastic deformation states of the contacting asperities. It is clearly seen that the high stiffness layer attains a maximum pressure ratio of 3.5 nearly at dimensionless interference of 3.0 which is more than the single asperity contact model limit of 2.8Y [12].It can be state that the elastoplastically deformed asperities start to interact among themselves and restrict the asperities further plastic deformation so the maximum pressure ratio increases beyond the hardness limit. In low stiffness and homogenous layer cases, the deformed asperities retain in elastoplastic states so the maximum pressure ratio is less than 2.8Y.

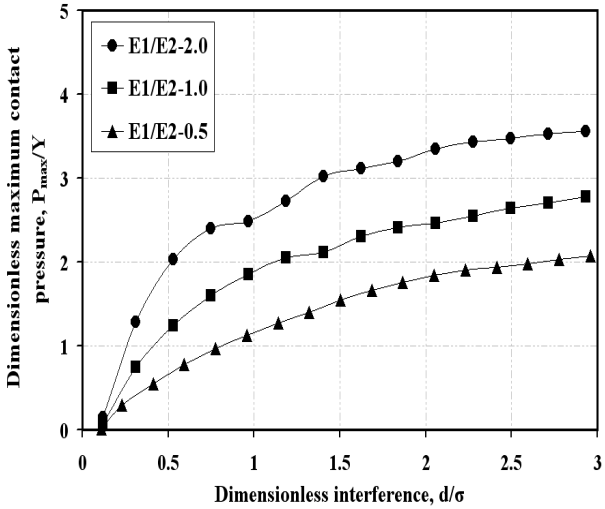

Fig. 7 Variation of dimensionless real area of contact with dimensionless contact load

Fig. 8 (a), (b) and (c) show von Mises stress plot obtained at the layer interface for all the three cases at dimensionless interference of 2.1. It is clearly seen in Fig. 8 (a) that the high stiffness layer holds more plastically yielded zone compared to the other cases. It is also noted that the interaction of asperities at surface level have certain influence on evolving contact stress at interface.

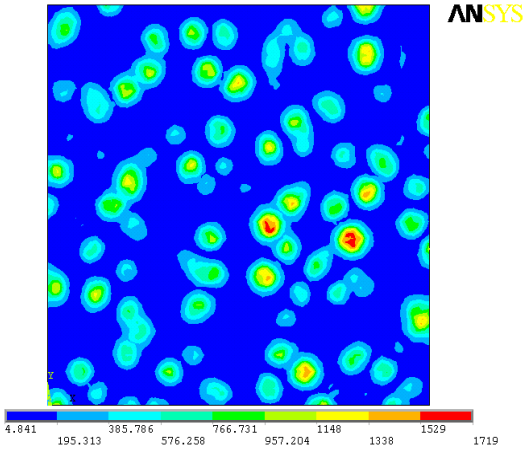

(a) E_1/E_2=1.0

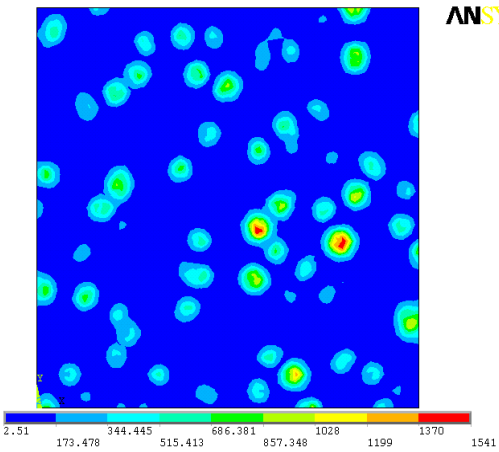

(b) E_1/E_2=1.0

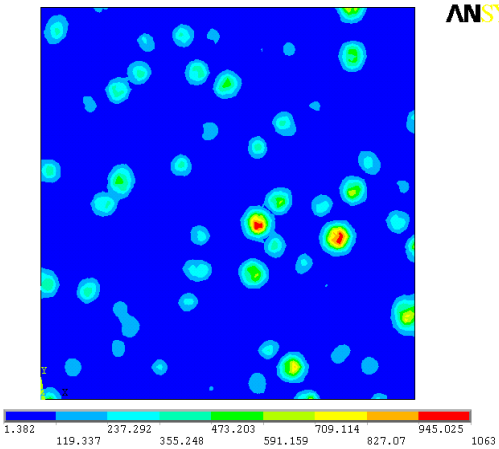

(c) E_1/E_2=0.5

Fig. 8 Von Mises stress plot at interface for d/σ of 2.1

V. Conclusion

A three dimensional finite element method based layered solid rough surface contact is developed. This approach can be substituted for conventional techniques of matrix inversion method and variation approach where the patch solution termination is achieved with a constant relation(H=2.8Y) but the present developed approach accounts the elastic, elastoplastic and plastic deformation of asperities with their continuity and adopts the arbitrary shape of asperities. It identifies the influence of neighbouring asperity interaction while finding the interfacial layer strength. A hard layer increases the effective hardness with less real area of contact.

Nomenclature

Ar	Real area of contact, μm^2
A_n	Nominal area of contact, μm^2
d	Interference, μm
E_1	Young's modulus of substrate material, *Gpa*
E_2	Young's modulus of layer material, *Gpa*
E^*	$E_2/(1-\nu_2)$, *Gpa*
h	Layer thickness, μm
H	Hardness
P_n	Contact load, *N*
Y_1	Yield strength of substrate material, *Gpa*
Y_2	Yield strength of layer material, *Gpa*
ν_1	Poisson's ratio of substrate material
ν_2	Poisson's ratio of layer material
σ	Standard deviation of rough surface, μm

References

[1] T. Merriman, and J. Kannel, "Analyses of the role of surface roughness on contact stresses between elastic cylinders with and without soft surface coating," ASME J.Tribol., vol. 111, pp. 87-94, 1989.
[2] T. Nogi, and T. Kato, "Influence of a hard surface layer on the limit of elastic contact .Part I. Analysis using a real surface model," ASME J. Tribol., vol. 119, pp. 493-500, 1997.
[3] M. R. Hestenes, and E. Stiefel, "Methods of conjugate gradients for solving linear systems," J. Res. Nat. Bur. Stand., vol. 49, pp. 409-436, 1952.
[4] R. Winther, "Some superlinear convergence results for the conjugate gradient method," Soc. Ind. Appl. Math. J. Numer., vol. 17, pp. 14-17, 1980.
[5] X. Tian, and B. Bhushan, "A numerical three-dimensional model for the contact of rough surfaces by variational principle," ASME J. Tribol., vol. 118, pp. 33–41, 1996.
[6] W. Peng, and B. Bhushan, "A numerical three dimensional model for the contact of layered elastic/plastic solids with rough surfaces by a variational principle," ASME J. Tribol., vol. 123, pp. 330-342, 2001.
[7] K. Komvopoulos, and N. Ye, "Three dimensional contact analysis of elastic-plastic layered media with fractal surface topographies," ASME J. Tribol., vol. 123, pp. 632-640, 2001.
[8] Z.Q. Gong, and K. Komvopoulos, "Effect of surface patterning on contact deformation of elastic-plastic layered media," ASME J. Tribol., vol. 125, pp. 16-24, 2003.
[9] Y. Z.Hu, and K. Tonder, "Simulation of 3D random rough surface by 2D digital filter and Fourier analysis," Int. J. Mach. Tools Manufact., vol. 32, pp. 83-90, 1992.
[10] T. W. Kim, B. Bhushan and Y.J. Cho, "The contact behavior of elastic/plastic non Gaussian rough surfaces," Tribology Letters, vol. 22, pp. 1-13, 2006.
[11] S. Cai, and B. Bhushan, "A numerical three dimensional contact model for rough, multilayered elastic/plastic solid surfaces," Wear vol. 259, pp. 1408-1423, 2005.
[12] L. Kogut and I. Etsion, "Elastic plastic contact analysis of sphere and a rigid flat," J. Appl. Mech. Trans., ASME, vol. 69, pp. 657-662, 2002.
[13] D. Tabor, "The hardness of materials," Oxford:Clarendon press,1951.